

PREDICTION OF THE LONGITUDINAL TENSILE STRENGTH OF POLYMER MATRIX COMPOSITES

A. B. de Morais

University of Aveiro, Department of Mechanical Engineering,
Campus Santiago, 3810-193 Aveiro, Portugal

Abstract

A micromechanical model was developed for the prediction of the longitudinal tensile strength of polymer matrix composites. The model considers successive fibre breaks within an infinitely wide L_i -long representative volume element (RVE), L_i being the so-called ineffective length. An elastic-plastic stress transfer model is used to define L_i and fibre strength is described by a Weibull distribution. The composite strength is obtained by solving numerically an equation for the maximum RVE stress. A simplified closed-form solution derived proved to be in very good agreement with the base formulation. Although there is still significant uncertainty over model input data, predictions agreed well with experimental strengths of carbon fibre composites.

Keywords: Polymer-matrix composites, longitudinal tensile strength, ineffective length, Weibull distribution.

1. Introduction

Laminated polymer matrix composites are increasingly used in structural applications. This is mainly due to the outstanding fibre dominated ply longitudinal modulus and tensile strength. It is well known that, in contrast with

matrix cracking, fibre fracture usually causes overall laminate failure. It is also known that modern structural design methodologies aim at taking full advantage of material properties. Therefore, accurate prediction of the ply longitudinal tensile strength, σ_{ul} , is an important contribution to avoid large safety factors. However, longitudinal failure is a complicated process [1-6].

Let us consider a unidirectional composite subjected to a rising tensile load. Owing to the statistical distribution of fibre strength, various fibre breaks occur at different locations. Broken fibres cannot support any load at the fractured section. However, shear stresses in the surrounding matrix gradually transfer stress to broken fibres. These fibres can actually recover the stress acting on unbroken fibres at some length L_i , known as “ineffective length”. Early strength prediction models have viewed the composite as a chain of L_i -bundles [1-6]. However, oversimplifying assumptions have been made to maintain analytical tractability. In order to overcome these limitations, Monte Carlo simulations have recently become widespread [7-14]. The models may contain hundreds of fibre elements, but computational cost limits model dimensions and thus makes further size scaling essential to predict σ_{ul} . Moreover, model predictions overestimate significantly experimental σ_{ul} values.

This paper presents a simplified model that compares favourably with experimental data for several carbon fibre composites.

2. Model description

The aim of the present model is to predict the longitudinal tensile strength of an infinite composite. In these circumstances, the composite can be seen as an infinite stack of L_i -long infinitely wide regions. Obviously, any of such regions can be considered the representative volume element (RVE). Therefore, the analysis yields the longitudinal tensile strength without requiring any further size scaling. Moreover, one fibre only undergoes a single break, thus greatly simplifying the analysis [14]. Failure occurs when the number of fibre breaks prevents further load increases.

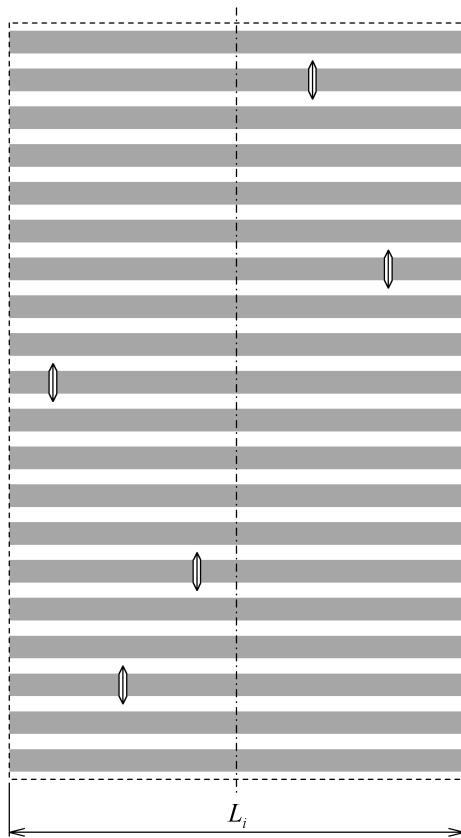


Figure 1: Fibre breaks in the RVE.

Early work by Hedgepeth [15,16] indicated that fibres adjacent to a broken one would be subjected to significant stress concentration effects. Most Monte Carlo simulations based models have included such effects and therefore predict the formation of broken fibre clusters. Furthermore, one of the clusters becomes unstable and triggers final failure [7-14]. Clusters of fibre breaks have been reported in model composites containing a very limited number of fibres [17]. They could also occur in contacting fibres of real composites, although they have not been observed in bundle tests [14]. In particular, the formation of one large cluster of fibre breaks leading to final failure seems unlikely and clearly lacks experimental support [14]. Moreover, three-dimensional finite element analyses showed very modest highly localised stress concentration in fibres adjacent to a broken fibre [18-20]. Therefore, it is assumed that fibre breaks are uniformly distributed in the RVE. This implies that the average axial distance of the breaks to the RVE mid-plane is $L_i/4$. The average stress supported by broken fibres in any transverse plane is thus the stress at $L_i/4$ from the fibre break. The RVE average fibre stress can then be expressed as

$$\sigma_{fa} = \sigma_{fl} [1 - P(\sigma_{fl})] + P(\sigma_{fl}) \sigma_{fb}(L_i/4) \quad (1)$$

where σ_{fl} and σ_{fb} are the stresses on the unbroken and broken fibres, respectively, and P is the cumulative probability of fibre failure. The two-parameter Weibull distribution is known to provide a good fit to experimental fibre strength data [21-23]. Thus, at gauge length L_i ,

$$P(\sigma_{fl}) = 1 - \exp \left[-L_i \left(\frac{\sigma_{fl}}{\sigma_{fi}} \right)^\rho \right] \quad (2)$$

where σ_{fi} is a characteristic strength and ρ the Weibull modulus. Since it is not possible to perform tensile tests at such small gauge lengths, the distribution of fibre strength must be scaled down from

experimental data for some larger gauge length L_0 ,

$$\sigma_{f_i} = \sigma_{f_0} \left(\frac{L_0}{L_i} \right)^{1/\rho} \quad (3)$$

This scaling seems to be reasonably accurate [21-23], although it tends to overestimate strength at small gauge lengths [23]. However, this can be explained by premature near the grips failure [22]. Eq. (2) is thus re-written as

$$P(\sigma_{f_i}) = 1 - \exp \left[- \frac{L_i^2}{L_0} \left(\frac{\sigma_{f_i}}{\sigma_{f_0}} \right)^\rho \right] \quad (4)$$

It is now necessary to determine L_i , which is strongly influenced by interface and matrix shear strengths. In general, interface debonding takes place when the interface is weaker than the matrix, while localised matrix cracking and yielding occur otherwise [19]. Recent experimental studies [24-26] suggest that matrix yielding is the main stress transfer mechanism in modern composite systems with treated and sized fibres. Accordingly, perfect interface bonding is assumed and L_i is calculated from the stress transfer model presented in [19]. This model is based on the analysis of a concentric cylinder cell formed by the broken fibre and the surrounding matrix layer (Fig. 2). The outer diameter of the matrix layer is tangent to the nearest neighbour fibres of the hexagonal packing arrangement, which is the most representative for the usual range of fibre contents. The thickness of the matrix layer is

$$t_m = d_f \left(\sqrt{\frac{\pi\sqrt{3}}{6V_f}} - 1 \right) \quad (5)$$

where d_f is the fibre diameter and V_f the fibre volume fraction. The matrix is assumed elastic-perfectly plastic with shear yield stress τ_{pm} . Neglecting normal stresses, stress transfer along the matrix yielding zone ($0 \leq z \leq z_p$) is [19]

$$\sigma_{f_b} = \frac{4\tau_{pm}}{d_f} z \quad (6)$$

In the subsequent elastic zone ($z \geq z_p$) [19],

$$\sigma_{f_b} = \sigma_{f_i} - \frac{4\tau_{pm}}{\beta d_f} e^{\beta(z_p - z)} \quad (7)$$

where

$$\beta = \sqrt{\frac{4G_m}{d_f t_m E_f}} \quad (8)$$

and G_m and E_f are the matrix shear modulus and the fibre longitudinal modulus, respectively. Stress continuity at z_p leads to

$$z_p = \frac{d_f \sigma_{f_i}}{4\tau_{pm}} - \frac{1}{\beta} \quad (9)$$

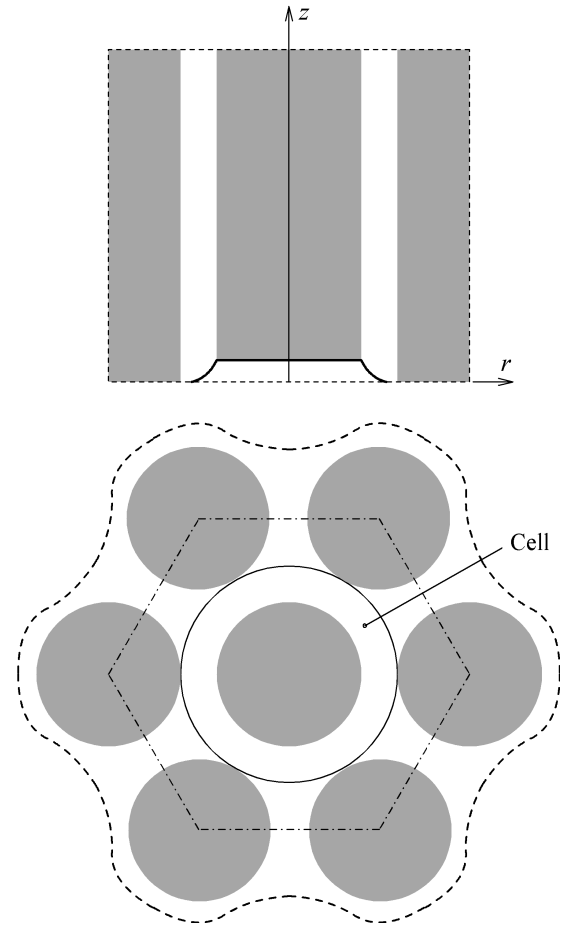


Figure 2: Scheme of the stress transfer model.

On the other hand, at $z = L_i$ the broken fibre recovers a high fraction α of the remote stress σ_{f_i} , e.g. $\alpha = 95\%$. Eqs. (7) and (9) allow us to write

$$L_i = \frac{d_f \sigma_{fl}}{4\tau_{pm}} \quad (10)$$

$$L_i \approx \frac{d_f \sigma_{fl}}{4\tau_{pm}} \quad (18)$$

$$-\frac{1}{\beta} \left\{ 1 + \ln \left[\frac{(1-\alpha)\beta d_f \sigma_{fl}}{4\tau_{pm}} \right] \right\}$$

Finally, we can determine the maximum fibre stress in the RVE from

$$\frac{d\sigma_{fa}}{d\sigma_{fl}} = 0 \quad (11)$$

After substitution of (4), (6) and (10), Eq. (11) can be expressed as

$$F_l(\sigma_{fl}) + F_b(\sigma_{fl}) = 0 \quad (12)$$

where

$$F_l(\sigma_{fl}) = \left[1 - \frac{\rho L_i^2}{L_0} \left(\frac{\sigma_{fl}}{\sigma_{f0}} \right)^\rho - \frac{2L_i \sigma_{fl}^{\rho+1} L'_i}{L_0 \sigma_{f0}^\rho} \right] H \quad (13)$$

and

$$F_b(\sigma_{fl}) = \frac{\tau_{pm} L'_i}{d_f} - \frac{\tau_{pm}}{d_f} \left[\frac{dL_i}{d\sigma_{fl}} - \frac{\rho L_i^3 \sigma_{fl}^{\rho-1}}{L_0 \sigma_{f0}^\rho} - \frac{2L_i^2 L'_i}{L_0} \left(\frac{\sigma_{fl}}{\sigma_{f0}} \right)^\rho \right] H \quad (14)$$

are the contributions of unbroken and broken fibres, respectively, and

$$L'_i = \frac{dL_i}{d\sigma_{fl}} \quad (15)$$

$$H = \exp \left[-\frac{L_i^2}{L_0} \left(\frac{\sigma_{fl}}{\sigma_{f0}} \right)^\rho \right] \quad (16)$$

Eq. (12) can be solved by a simple numerical procedure e.g. Newton's method. The result is then inserted in (1) and the tensile strength calculated from the rule-of-mixtures

$$\sigma_{ut1} \approx V_f \sigma_{fa} \quad (17)$$

If we neglect:

- the contribution of broken fibres to the RVE stress;
- the stress transfer along the matrix elastic zone, and thus assume that

we obtain the closed-form equation

$$\sigma_{ut1} = V_f \left[\frac{16\tau_{pm}^2 L_0 \sigma_{f0}^\rho}{(\rho+2)d_f^2} \right]^{\frac{1}{\rho+2}} e^{-1/(\rho+2)} \quad (19)$$

which is quite convenient if validated by the base model.

3. Results and discussion

The developed model is applied below to carbon fibre composites. The first objective was to evaluate the accuracy of the closed-form Eq. (19) in the usual range of material properties.

Epoxy resins have tensile moduli between 3.5 and 4.3 GPa and Poisson ratios from 0.35 to 0.42. Therefore, one can expect shear moduli G_m from 1.2 to 1.6 GPa, which a narrow interval. On the other hand, tensile strengths σ_{pm} vary from 60 to 100 MPa, but shear strength data is scarce and somewhat controversial. The von Mises type relation $\tau_{pm} = 0.577\sigma_{pm}$ has often been employed, but there substantial evidence that polymers actually undergo local tensile failure under shear loadings [27-31]. Accordingly, it is assumed here that $\tau_{pm} \approx \sigma_{pm}$.

As mentioned above, measuring parameters of the statistical fibre strength distributions is difficult at small gauge-lengths. Nevertheless, recent single fibre tensile tests on wide variety of carbon fibres showed Weibull moduli $\rho = 4$ to 6 [21]. For the most common carbon fibres (T300, T800 and AS4), $\rho \approx 5$ [13,32,33], the value that is used here.

Comparison between Eq. (19) and the base formulation was first made in 4 cases, which correspond to the combinations of 2 fibres (WF and SF) and 2 matrices (WM and SM). The fibres used were:

- WF with $d_f = 7 \mu\text{m}$, $E_f = 230 \text{ GPa}$ and $\sigma_{f0} = 3500 \text{ MPa}$ for $L_0 = 15 \text{ mm}$;
- SF having $d_f = 5 \mu\text{m}$, $E_f = 300 \text{ GPa}$ and $\sigma_{f0} = 7000 \text{ MPa}$ for $L_0 = 15 \text{ mm}$;

properties that bound those of well known Toray's T300 and T800 fibres. The softer WM matrix had $G_m = 1.2 \text{ GPa}$ and $\tau_{pm} = 40 \text{ MPa}$, while $G_m = 1.6 \text{ GPa}$ and $\tau_{pm} = 100 \text{ MPa}$ were assumed for the stronger WM.

Fig. 3 shows that Eq. (19) is in very good agreement with the base model for all cases considered. Therefore, it was used for comparison with experimental data.

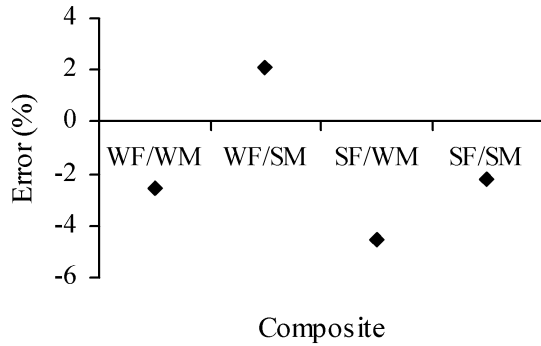


Figure 3: Errors (%) of Eq. (19) in the 4 cases considered (see text for details).

The present model is now applied to Hexcel AS4 and Toray T300 carbon fibre composites, since there is considerable experimental data in the literature and material supplier datasheets (Tables 1 and 2). Data sources are Cytec, Hexcel, Matweb, Qinetiq and Soficar. The fibre volume fraction V_f was estimated from the composite-to-fibre moduli ratio, E_1/E_f .

At this stage, the main difficulty in model evaluation is the lack of reliable data for the fibre characteristic strength σ_{f0} . Nevertheless, it is possible to evaluate the model by the following procedure:

- use experimental σ_{ut1} values and Eq. (19) to back-calculate σ_{f0} for some pre-defined L_0 ; similar values should be

obtained for the composites with the same fibres;

- apply Eq. (19) with the average σ_{f0} values obtained previously.

Composite design.	Matrix	V_f	σ_{pm} [MPa]	σ_{ut1} [MPa]
A1	828m	0.59	90	1890
A2	828m	0.64	90	2044
A3	934	0.54	83	1586
A4	934	0.60	83	1792
A5	997	0.57	90	1930
A6	997	0.63	90	2206
A7	8551.7	0.63	97	2170
A8	APC2	0.58	100	2060
A9	APC2	0.66	100	2297

Table 1: Experimental data of AS4 fibre composites used for model evaluation.

Composite design.	Matrix	V_f	σ_{pm} [MPa]	σ_{ut1} [MPa]
T1	3601	0.59	60	1575
T2	3631	0.59	90	1740
T3	934	0.60	83	1790
T4	914	0.60	48	1432
T5	924	0.60	65	1698
T6	3631	0.57	90	1760

Table 2: Experimental data of T300 fibre composites used for model evaluation.

Results presented in Fig. 4 for $L_0 = 10 \text{ mm}$ confirm that consistent σ_{f0} values could be back-calculated. The largest error was -11.7% for an AS4 composite. As expected, calculated σ_{f0} values were higher than those of single fibre tests [32,33]. This is due to the high stress transfer effects that lead to premature near the grips failure.

Finally, Figs. 5 and 6 show that model predictions agree quite well with the experimental data of Tables 1 and 2.

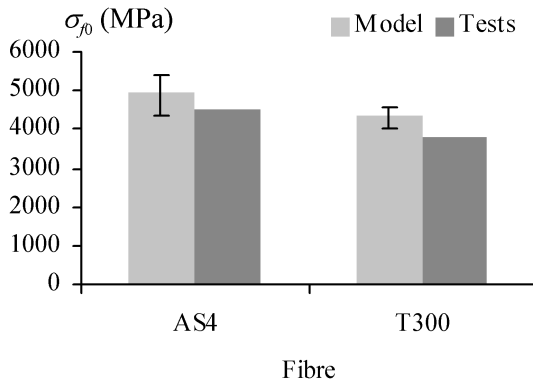


Figure 4: Calculated (see text) and measured [32,33] characteristic fibre strengths.

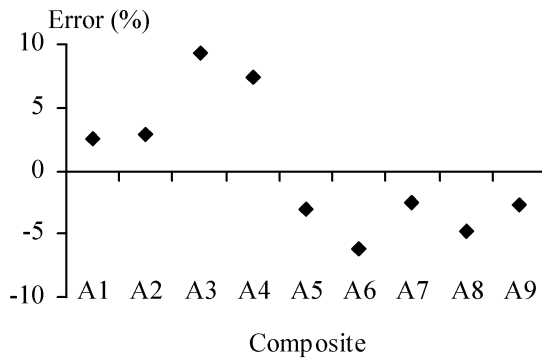


Figure 5: Errors (%) of Eq. (19) predictions relative to experimental data of AS4 composites (Table 1).

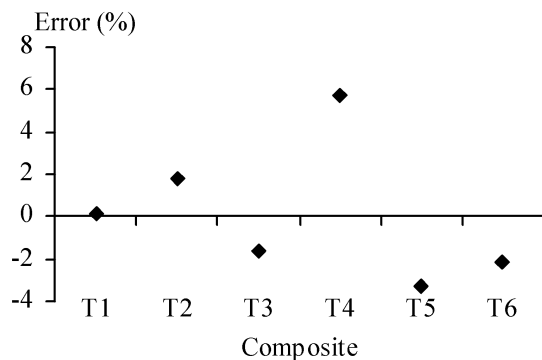


Figure 6: Errors (%) of Eq. (19) predictions relative to experimental data of T300 composites (Table 2).

4. Conclusions

A micromechanical model was presented in this paper for predicting the longitudinal tensile strength of polymer matrix composites. The model considered an infinitely wide L_i -long representative volume element (RVE), L_i being the so-called ineffective length. Its value was calculated from an elastic-plastic stress transfer model previously developed by the author. Fibre strength was assumed to follow a Weibull distribution and therefore, under increasing load, various fibres breaks take place in the RVE. Tensile strength can be obtained by solving numerically an equation for the maximum RVE stress. An additional closed-form solution was obtained by neglecting the contribution of broken fibres and the elastic stress transfer length. A preliminary parametric study showed that the closed-form solution gave very good approximations to the base formulation.

The present model allowed back-calculation of consistent fibre characteristic strengths from experimental data of AS4 and T300 carbon fibre composites. Moreover, strength predictions agreed quite well with experimental values.

References

1. Rosen, B.W., (1964), *AIAA J*, **2**, pp. 1982-1991.
2. Zweben, C., Rosen, B.W., (1970), *J Mech Phys Solids*, **18**, pp. 180-206.
3. Harlow, D.G., Phoenix, S.L., (1978), *J Compos Mater*, **12**, pp. 195-214.
4. Batdorf, S.B., (1982), *J Reinf Plastics Compos*, **1**, pp. 153-164.
5. Phoenix, S.L., Smith, R.L., (1983), *Int J Solids Struct*, **19**, pp. 479-496.
6. Harlow, D.G., Phoenix, S.L., (1991), *J Mech Phys Solids*, **39**, pp. 173-200.
7. Curtin, W.A., Takeda, N., (1998), *J Compos Mater*, **32**, pp. 2042-2059.

8. Curtin, W.A., Takeda, N., (1998), *J Compos Mater*, **32**, pp. 2060-2081.
9. Mahesh, S., Beyerlein, I.J., Phoenix S.L., (1999), *Physica*, **D133**, pp. 371-389.
10. Landis, C.M., Beyerlein, I.J., McMeeking, R.M., (2000), *J Mech Phys Solids*, **48**, pp. 621-648.
11. Okabe, T., Takeda, N., Kamoshida, Y., Shimizu, M., Curtin, W.A., (2001), *Compos Sci Technol*, **61**, pp. 1773-1787.
12. Okabe, T., Takeda, N., (2002), *Composites Part A*, **33**, pp. 1327-1335.
13. Okabe, T., Takeda, N., (2002), *Compos Sci Technol*, **62**, pp. 2053-2064.
14. Mahesh, S., Phoenix, S.L., Beyerlein, I.J., (2002), *Int J Fract*, **115**, pp. 41-85.
15. Hedgepeth, J.M., (1961), NASA-TND-882.
16. Hedgepeth, J.M., Van Dyke, P., (1967), *J Compos Mater*, **1**, pp. 294-309.
17. Aroush, D.R.-B., Maire, E., Gauthier, C., Youssef, S., Cloetens, P., Wagner, H.D., *Compos Sci Technol*, in Press.
18. Nedele, M.R., Wisnom, M.R., (1994), *Compos Sci Technol*, **51**, pp. 517-524.
19. de Morais, A.B., (2001), *Compos Sci Technol*, **61**, pp. 1571-1580.
20. van den Heuvel, P.W.J., Goutianos, S., Young, R.J., Peijs, T., (2004), *Compos Sci Technol*, **64**, pp. 645-656.
21. Tagawa, T., Miyata, T., (1997), *Mater Sci Engng*, **A238**, pp. 336-342.
22. Pickering, K.L., Bader, M.G., Kimber, A.C., (1998), *Composites Part A*, **29A**, pp. 435-441.
23. Pickering, K.L., Murray, T.L., (1999), *Composites Part A*, **30A**, pp. 1017-1021.
24. Deng, S., Ye, L., Mai, Y.W., Liu, H.Y., (1998), *Composites Part A*, **29A**, pp. 423-434.
25. van den Heuvel, P.W.J., Wubbolts, M.K., Young, R.J., Peijs, T., (1998), *Composites Part A*, **29A**, pp. 1121-1135.
26. van den Heuvel, P.W.J., Peijs, T., Young, R.J., (2000), *Composites Part A*, **31A**, pp. 161-171.
27. Chai, H., (1988), *Int J Fract*, **37**, pp. 137-159.
28. Chai, H., (1993), *Int J Fract*, **60**, pp. 311-326.
29. O'Brien, T.K., (1998), In: ASTM STP 1330, pp. 3-18.
30. Liu, K., Piggott, M.R., (1998), *Polym Engng Sci*, **38**, pp. 60-68.
31. Liu, K., Piggott, M.R., (1998), *Polym Engng Sci*, **38**, pp. 69-78.
32. Fukuda, H., Miyazawa, T., (1994), *Adv Compos Mater*, **4**, pp. 101-110.
33. Beyerlein, I.J., Phoenix, S.L., (1996), *Compos Sci Technol*, **56**, pp. 75-92.